

# Room-Temperature Magnetism in the Crystal of a 1,6-Heptadiyne Derivative and the Processable Polymer

Manyu Chen<sup>1</sup>, Guangze Hu<sup>1</sup>, Zuping Xiong<sup>1</sup>, Haoyuan Hu<sup>1</sup>, Jing Zhi Sun<sup>1,2\*</sup>, Haoke Zhang<sup>1,3\*</sup>, Ben Zhong Tang<sup>1,4\*</sup>

<sup>1</sup> MOE Key Laboratory of Macromolecules Synthesis and Functionalization, Department of Polymer Science and Engineering, Zhejiang University, Hangzhou 310058, China. E-mail: [sunjz@zju.edu.cn](mailto:sunjz@zju.edu.cn).

<sup>2</sup> Centre for Healthcare Materials, Shaoxing Institute, Zhejiang University, Shaoxing 312000, China.

<sup>3</sup> Hangzhou Global Scientific and Technological Innovation Centre, Zhejiang University, Hangzhou 311215, China. E-mail: [zhanghaoke@zju.edu.cn](mailto:zhanghaoke@zju.edu.cn).

<sup>4</sup> Shenzhen Institute of Molecular Aggregate Science and Engineering, School of Science and Engineering, The Chinese University of Hong Kong, Shenzhen 518172, China. E-mail: [tangbenz@cuhk.edu.cn](mailto:tangbenz@cuhk.edu.cn).

Keywords: organic magnets, room-temperature magnetism, radical, polymer

## Abstract

Room-temperature organic magnetic materials have been a sought-after but challenging topic for a long time. Besides the reported organic-containing magnets including pure organic radicals, charge-transfer salts, and coordination polymers, we report a novel and alternative approach to fabricate purely organic/polymeric magnets based on the crystal of a 4-substituted 1,6-diyne (M1) and its polymer (P1). Both of the white M1 crystal and the black P1 powder samples exhibit room-temperature magnetism. The saturation magnetization of P1 is about 0.25 emu g<sup>-1</sup> and its Curie temperature is higher than 400 K. After repeated recrystallization of M1 and precipitation of P1 to thoroughly remove the metal-catalyst residues, the room-temperature magnetism of M1 and P1 is tentatively assigned to the stable radicals in the solid samples. The results demonstrated in this work suggest an unprecedented strategy to obtain room-temperature organic magnets.

## 1. INTRODUCTION

Magnetic materials have irreplaceable applications in many important areas such as information storage, quantum computing and spin sensors. Characterized by the traits of low density, easy processing and tailorabile chemical structure, organic/polymeric magnets have attracted more and more attention both in academic and industrial fields.<sup>[1-7]</sup> Although the prediction of the existence of the magnetic exchange interaction between  $\pi$ -electron spins in aromatic and olefinic free radicals was proposed by McConnell as early as in 1963,<sup>[8]</sup> the first magnetic polymer-(poly-BIPO) was contributed by Ovchinnikov and Spector et al. in 1987,<sup>[9]</sup> and the discovery of the first pure organic ferromagnet (*p*-nitrophenyl nitronyl nitroxide crystal) was reported by Takahashi and Turek et al. in 1991.<sup>[10]</sup> These pioneering works led to the development of this particular research field, and a series of magnetic organic compounds (e.g., nitroxide radicals, phenoxy radicals, and ammonium sulfate radicals) and polymers (e.g., polyarylmethylene, fullerene C<sub>60</sub> polymers, and poly(9,10-anthracene-acetylene) were emerged and documented.<sup>[11-20]</sup>

Despite these significant advances, most of the organic/polymer magnets have Curie temperatures far below room temperature and low stability, making them difficult to acquire practical application. In recent years, researchers have tried a variety of strategies to obtain room-temperature magnetic organic/polymeric materials with high Curie temperature and high stability. For example, in 2018, Huang and coworkers obtained a room-temperature ferromagnet by ultrasonic treatment and low-temperature annealing of naphthalene.<sup>[21]</sup> In 2022, Ma and colleagues reported a solvothermal

approach for the preparation of room-temperature ferromagnet from perylene diimide aggregates with a Curie temperature over 400 K.<sup>[22]</sup> In recent years, two-dimensional and framework constructions have been adopted for the design and synthesis of organic/polymeric magnetic materials, to enhance the thermal and structural stability of the free radical species.<sup>[23-30]</sup> For example, in 2012, Irena et al. reported the magnetic spin interaction in polymer aromatic amines by adjusting the  $\pi$ -conjugated system.<sup>[18]</sup> In 2018, Yoo and Baek et al. reported the highly stable free radicals achieved through the efficient self-polymerization of tetracyanoquinodimethane monomer.<sup>[23]</sup> 2019, Wu and colleagues described the synthesis of 1,3,5-triazine-linked porous organic radical frameworks by thermal or triflic acid assisted polymerization from the cyano-containing stable radical monomers.<sup>[24]</sup> Due to the magnetically radicals coupled with each other through the 1,3,5-triazine connector, the polymers exhibited spontaneous magnetization or super-paramagnetism at room temperature.

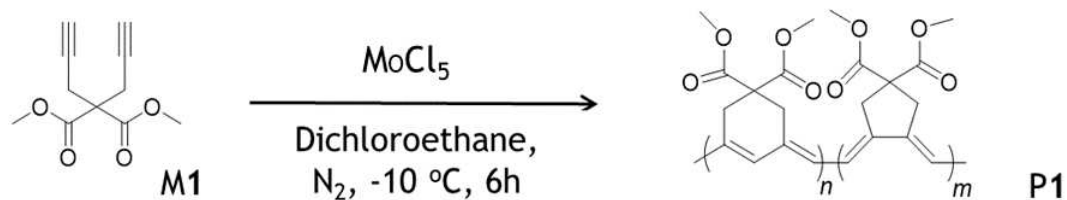
As theoretical prediction, polyacetylene with polyene backbone may have magnetic behavior.<sup>[31, 32]</sup> In fact, electron spin resonance (ESR) experimental data showed that the concentration of paramagnetic center in undoped trans-polyacetylene films was about  $3 \times 10^{19}$  spin/g, but such a spin density and the very low stability could not afford evident magnetism of intrinsic polyacetylene.<sup>[32]</sup> Inspired by the pioneer work of the magnetic polymer (poly-BIPO), a series of polyacetylene and polyyne derivatives modified with stable radicals were prepared and the concentration of radicals increased several orders of magnitude, the magnetic behavior suggested the presence of spin-glass.<sup>[33-40]</sup> Generally, the magnetism of these polymers comes from the pendant

polyradicals, because they accumulate radical molecules along one conjugated polymer chain. Up to now, the magnetic materials based on conjugated polymers including polyacetylenes still face three problems: (1) extrinsic magnetic property, the spin exchange origins from the radical modifiers but not the conjugated main chain; (2) poor stability, the magnetism disappears after being placed in the air for a period of time; (3) low Curie temperature, magnetic response loses at ambient temperature. In this work, we demonstrate room temperature magnetism of the powders of a polymer (P1) and the crystalline monomer of 4,4-bis-methoxycarbonyl-1,6-heptadiyne (M1). P1 showed a Curie temperature  $> 400$  K. The magnetic property can retain in dark and at ambient temperature for months. In addition, the free radicals are generated in polymer's backbone rather than introduced from the modification of the polymer with stable radical side chains.

## 2. RESULTS AND DISCUSSION

The chemical structures of the 1,6-diyne and its polymer, and the synthetic route are shown in Scheme 1. White crystals of the monomer (M1, 4,4-bis-methoxycarbonyl-1,6-heptadiyne) were obtained after recrystallization of the primary resultant (Scheme S1). The polymerization of M1 largely followed the procedures of metathesis cyclopolymerization, as described in literature.<sup>[41-43]</sup> Under the optimized reaction conditions, the poly(1,6-heptadiyne) derivative P1 was obtained in good yield by using transition metal catalyst  $\text{MoCl}_5$  in ultra-dry 1,2-dichloroethane (DCE) under nitrogen atmosphere, the optimization processes were described in Experimental section and Supporting Information (Table S1). The data of structure characterization of the

monomer and polymer are also presented in the experimental section and supporting information (Scheme S1, Table S1, Figures S1-S2)



**Scheme 1.** Synthetic route to poly(4,4-bismethoxycarbonyl-1,6-heptadiyne) (P1).

According to the characterization data, the expected monomer and polymer were successfully derived. A noticeable experimental phenominon was that the clear solution of M1 was turned into a dark red solution by the polymerization reaction. After purification, black powders of P1 was obtained (inset of Figure 1 and videos in Supporting Inforamtion). The UV-visible absorption spectra of M1 and P1 are displayed in Figure 1. In tetrahydrofuran (THF) solution, M1 has no absorption in the visible spectral region, while the absorption spectrum of P1 features by a very broad band ranging from 300 to 640 nm with an obtuse peak at around of 490 nm.

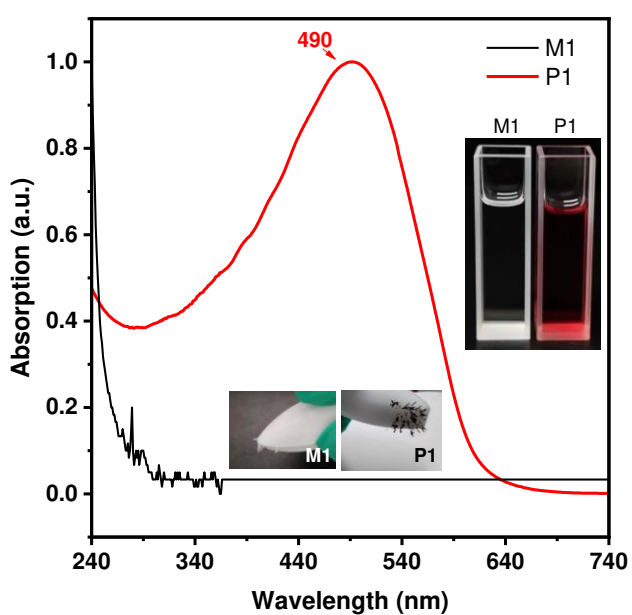


**Figure 1.** UV-visible absorption spectra of M1 and P1 in THF solution ( $1 \times 10^{-5}$  mol/L).

Inset photographs: right, M1 and P1 in THF solutions; bottom, powders of M1 and P1 attracted on the surface of magnetic stir bars.

A fortuitous observation was that M1 crystals could be attracted by the magnetic stir bar (inset photograph in Figure 1). After eliminated the electrostatic action, this observation was associated with magnetic effect, though it was weak. It is interesting that the magnetic property was also observed for the polymer resultant P1. In the purification process of P1 using dissolution and precipitation technique, it was observed that the black P1 powders were attracted by and closely adsorbed onto the surface of the magnetic stir bar (inset in Figure 1), and the magnetized powders could be adsorbed by an iron scissor (Video 2, Supporting Information). This phenomenon was observed in repeated dissolution and precipitation operation. After excluding out the leakage of the magnet component in stir bar by repeating a polymerization experiment, we ensured that the black powders are magnetic.

Since the magnetic behavior usually origins from the free radical species, the electron paramagnetic resonance (EPR) spectroscope of the crystals of M1 and powders of P1 was measured and the results are displayed in Figure 2. For M1, the EPR signals are weak but authentic (Figure 2A). The *g* factor is 2.0062, which is larger than free electron's (2.0023) and can be tentatively assigned to the organic free carbon radicals. The wide and unsymmetric peaks suggest that the free radicals are in a slowly relaxing and anisotropic environment. These features are consistent with the fact that the radicals are localized in anisotropic and stable crystalline arrays. For P1, a *g* factor of 2.0027

is recorded, and the resonance signals are relatively strong and largely symmetric as compared with M1. It means that the radicals in P1 powders are in a slowly relaxing and isotropic environment, the rigidity is smaller than and the activity is higher than that in crystals of M1. These features are consistent with the fact that P1 is an amorphous solid and it has a conjugated mainchain. The *g* values of M1 and P1 are much smaller than that of magnetic metals, implying that the magnetic behaviors do not result from metal species.

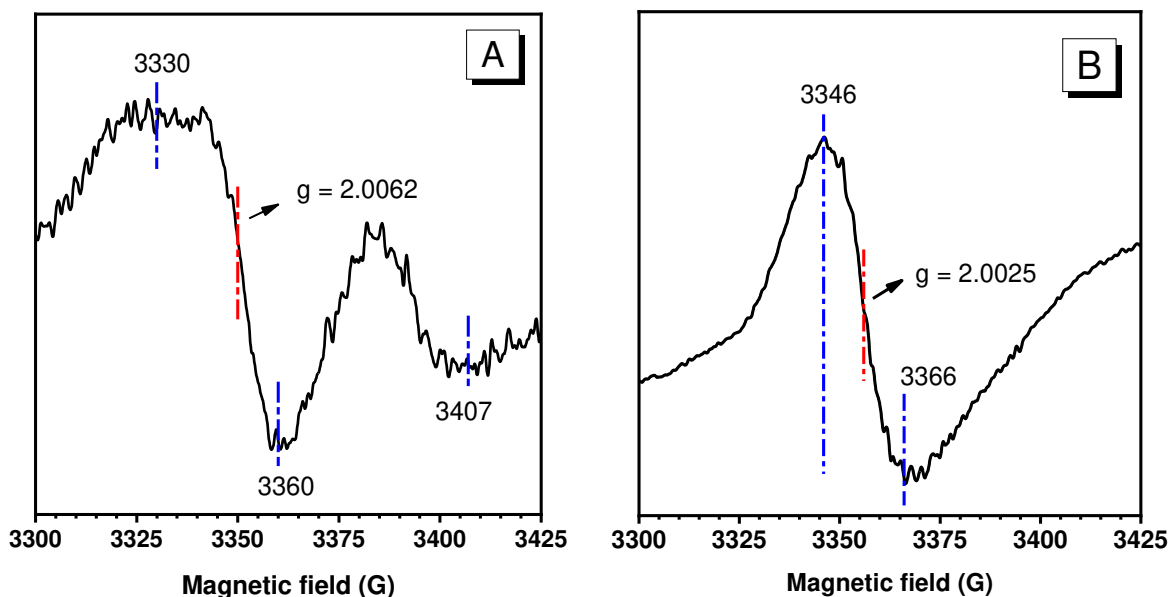


**Figure 2.** Electron paramagnetic resonance (EPR) spectra of M1 (A) and P1 (B) powders.

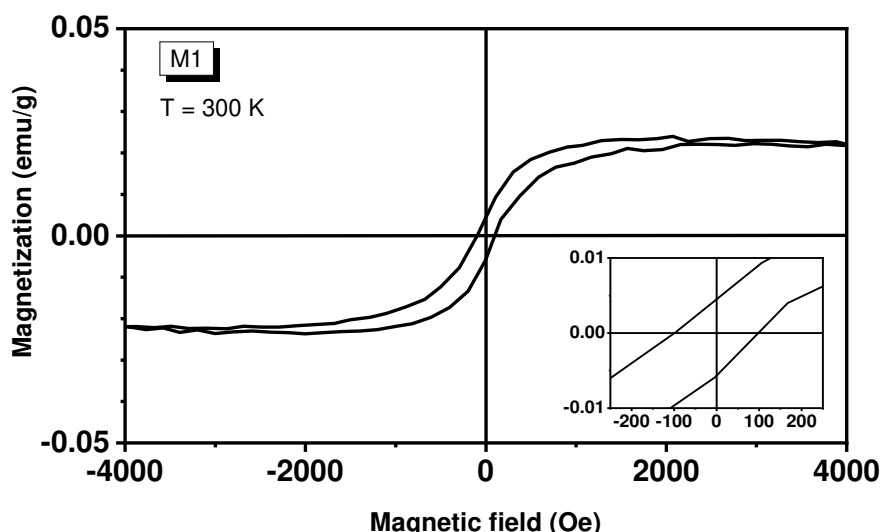


**Figure 3.** The magnetization–magnetic field (M–H) curves of M1 crystals (upper) and P1 powders (lower) measured at 300 K. The saturation magnetization for M1 and P1 is 0.025 and 0.25  $\text{emu g}^{-1}$ , respectively. Inset shows the amplified parts of the curves at around zero field.

To study the magnetism of M1 and P1, the magnetization–magnetic field (M–H) curves were recorded at 300 K, and the data are shown in Figure 3 and S3, the typical magnetic hysteresis loops can be obtained for both M1 and P1. For M1, the saturated magnetization is around 0.025  $\text{emu g}^{-1}$  at 300 K, indicating a very weak magnetic property. For P1, the saturated magnetization at 300 K was 0.25  $\text{emu g}^{-1}$ , which is 10 times of M1. This value is about 66 times large than that of 1,3,5-trizaine-linked porous organic radical frameworks ( $3.8 \times 10^{-3}$   $\text{emu g}^{-1}$ ) measured at room temperature [24]. Meanwhile, the temperature is higher than recently reported amorphous polymerized TCNQ framework (36 K) [30]. Moreover, P1 is soluble in some organic solvents such as THF and DMF, thus allow to be processed by solution casting and spincoating

techniques to fabricate self-supporting solid films, as displayed by the photographs in Figure S4. Accordingly, the magnetic property of P1 was carefully investigated. As demonstrated in Figure 3, the M–H curve reaches saturation magnetization at 7600 Oe and the coercive field reached 133.7 Oe at 300 K; the residual magnetism (Mr) and coercivity (Hc) of P1 is 0.01 emu g<sup>-1</sup> and 33.9 Oe, respectively.

Since metal catalysts containing Mo and Sn were used in the polymer preparation, the Mo-based compound residues (e.g., Molybdenum oxide) may cause the weak magnetic behavior. To eliminate the interference of metal impurities, the resultant polymer was purified by repeated precipitation treatment for several times and the content of molybdenum in P1 was lower than 0.02 %, as revealed by the data of inductively coupled plasma optical emission spectrometer (ICP-OES, Table S2). Such low Mo-content in P1 is not enough to cause the magnetization phenomenon shown in Figure 3 and the inset of Figure 1. Furthermore, both molybdenum chloride and oxide show diamagnetism property (Figure S5). Therefore, the results indicate that the magnetization phenomenon originates from P1 rather than metal-catalyst residues.

It is significant that the magnetic property could be tested at 300 K, this means the Curie temperature ( $T_c$ ) of P1 must be higher than room temperature. Then, we measured the magnetic susceptibility and Curie temperature of P1 by superconducting quantum interference device (SQUID) and physical property measurement system (PPMS) in the temperature range of 2–300 K under an external field and 0.5 T. The experimental results are shown in Figures 4 and S6. The temperature dependence of magnetic susceptibility ( $\chi$ ) suggests that P1 is a typical magnetic material, the maximum value

appears at about 206 K, indicating the best matching between the spin-alignment and applied field at this temperature (Figure S6 (a)).

The temperature-dependence of the product of magnetic susceptibility and temperature ( $\chi T$ ) gives a good linear relationship with a tendency of monotonous increase, and the  $\chi T$  value at 300 K is over 90 emu g<sup>-1</sup>T<sup>-1</sup>, which is reasonable for a weakly coupled radicals (Figure S6 (b)). Figure 4 displays the temperature dependence of magnetization in zero-field-cooled (ZFC) and field-cooled (FC) conditions under a magnetic field of 100 Oe. A bifurcation point between the plots of ZFC and FC can be seen at 400 K, indicating that the value of T<sub>c</sub> of the magnetic P1 powders should be no lower than 400 K, which is rarely observed for organic-polymeric magnetic materials.

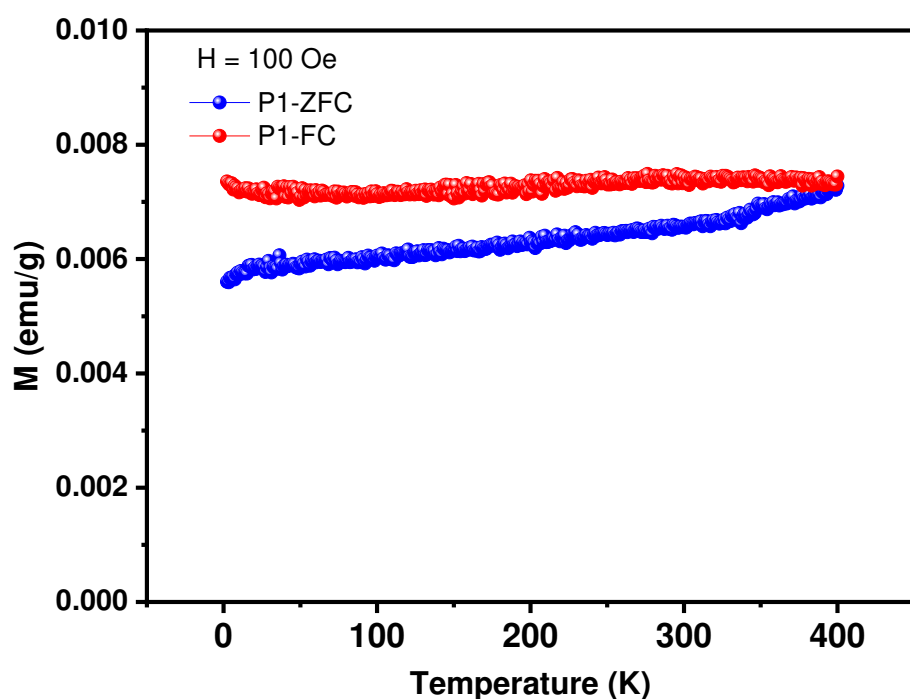


**Figure 4.** Temperature-dependent magnetic property of P1 powders: the plots of the variations of ZFC and FC magnetization intensity of P1 with temperature measured at an applied magnetic field of 100 Oe.

### 3. CONCLUSION

The crystals of 4,4-bis-methoxycarbonyl-1,6-heptadiyne (M1) and its polymer (P1) show distinct magnetism and stable electron paramagnetic signals at ambient temperature. The results of magnetic measurements indicate that both of M1 and P1 possess room-temperature magnetism. P1 powders possess a Curie temperature of at least 400 K and a saturation magnetization of 0.25 emu g<sup>-1</sup>. The interference from the metal-catalyst residues has been full removed and the magnetism of P1 can be tentatively ascribed to the intrinsic radicals in the conjugated polymer chains. In addition to the obvious magnetism, P1 exhibits the solution-processablility, a unique property of the polymer materials. The findings in this work imply that the room-temperature magnetism could be achieved by rational polymer design, it furnishes an alternative approach to fabricate pure organic-polymeric materials with room-temperature magnetism.

### 4. EXPERIMENTAL SECTION

#### 4.1. Materials

Dimethyl malonate was purchased from Bidepharm, propargyl bromide was purchased from Macklin, sodium hydride (NaH), 1-(3-dimethylaminopropyl)-3-ethylcarbodiimide hydrochloride, 4-dimethyl-aminopyridine (DMAP), ultra-dry tetrahydrofuran (THF) and ultra-dry 1,2-dichloroethane (DCE) were purchased from J&K Scientific, molybdenum chloride (MoCl<sub>5</sub>) was purchased from Sigma Alarich, and tetra-*n*-butyltin (*n*-Bu<sub>4</sub>Sn) was purchased from Alfa Aesar. Anhydrous methanol (MeOH) and potassium hydroxide (KOH), ammonium chloride (NH<sub>4</sub>Cl) and anhydrous

sodium sulfate ( $\text{Na}_2\text{SO}_4$ ) were purchased from Sinopharm. All chemicals are used directly without further purification.

#### 4.2. Instruments

The molecular weight ( $M_w$  and  $M_n$ ) and polydispersity ( $M_w/M_n$ ) of the polymer were estimated in THF using a gel permeation chromatography (GPC, PL-GPC-50, Waters Corporation, Milford, CT, USA) system with a set of monodisperse polystyrene standards covering the molecular weight varying from  $10^3$  to  $10^7$  as calibration. FTIR spectra were recorded on a VECTOR 22 (Bruker Corporation, Billerica, MA, USA) spectrometer.  $^1\text{H}$  NMR spectra were recorded on AVANCE III 400 (Bruker Corporation, Billerica, MA, USA) spectrometers, and tetramethylsilane (TMS) was used as an internal standard. UV-vis absorption spectra were recorded on a Varian CARY 100 Bio UV-vis (Agilent Technologies Inc, Santa Clara, CA, USA) spectrophotometer. The free radical signal was tested by Bruker's Brooke EMXplus-9.5/12 device (Bruker EMXplus EPR Spectrometer). The room temperature magnetization curve was tested by VersaLab (produced by Quantum Design, USA). The variable temperature magnetic susceptibility curve and ZFC-FC curve were tested using PPMS-9 (produced by Quantum Design in USA).

#### 4.3. Polymer preparation

In the glove box, 0.01 mol of catalyst ( $\text{MoCl}_5$ ) was weighed in the polymerization tube, 0.02 mol of tetrabutyltin was taken with a micro-injector after the catalyst was added, and then 1 mL of DCE solvent was added. In another polymerization tube, 0.5 mol of monomer was weighed, 1 mL of ultra-dry DCE was added to dissolve the

monomer, and then the monomer solution was transferred to the polymerization tube where the catalyst had been activated for 15 min. At the end of the reaction at the preset temperature and time, 1 mL of methanol was added to terminate the reaction, and then the solution was then dropped into a large amount of methanol through a glass dropper and precipitated overnight. The resultant was filtered using a sand core funnel. The resultant was purified with repeated dissolving and precipitation operations for no less than 6 times, and the precipitate was dried in vacuum dry to a constant weight, and finally black powder (P1) was obtained. The synthetic procedures of the monomer and the structure characterization data of the monomer and polymer are included in Supporting Information.

## **CONFLICT OF INTEREST**

There are no conflicts of interest to declare.

## **ACKNOWLEDGMENT**

This work was financially supported by the Natural Science Foundation of China (Nos. 22071215 and 52350002).

## **SUPPORTING INFORMATION**

Supporting Information is available from the Wiley Online Library or from the authors.

## **REFERENCES**

1. R. M. White, *Science* **1985**, 229, 11.

2. J. S. Miller, *Adv. Mater.* **1994**, 6, 322.
3. M. Kamachi, *J. Macromol. Sci., Polym. Rev.* **2002**, C42, 541.
4. A. Rajca, *Chem. Eur. J.* **2002**, 8, 4834.
5. S. J. Blundell, F. L. Pratt, *J. Phys-condens. Mat.* **2004**, 16, R771.
6. P. Bujak, I. Kulszewicz-Bajer, M. Zagorska, V. Maurel, I. Wielgus, A. Pron, *Chem. Soc. Rev.* **2013**, 42, 8895.
7. J. S. Miller, *Pramana* **2006**, 67, 1.
8. H. M. McConnell, *J. Chem. Phys.* **1963**, 39, 1910.
9. Y. V. Korshak, T. V. Medvedeva, A. A. Ovchinnikov, V. N. Spector, *Nature* **1987**, 326, 370.
10. M. Takahashi, P. Turek, Y. Nakazawa, M. Tamura, K. Nozawa, D. Shiomi, M. Ishikawa, M. Kinoshita, *Phys. Rev. Lett.* **1991**, 67, 746.
11. E. Coronado, C. Giménez-Saiz, C. J. Gómez-García, F. M. Romero, A. Tarazón, *J. Mater. Chem.* **2008**, 18, 929.
12. C. Paulsen, J. Souletie, P. Rey, J. Magn. Magn. Mater. **2001**, 226, 1964-1966.
13. F. M. Romero, R. Ziessel, M. Drillon, J. L. Tholence, C. Paulsen, N. Kyritsakas, J. Fisher, *Adv. Mater.* **1996**, 8, 826.
14. T. Kaneko, K. Iwamura, R. Nishikawa, M. Teraguchi, T. Aoki, *Polymer* **2014**, 55, 1097.
15. M. Mitani, D. Yamaki, Y. Yoshioka, K. Yamaguchi, *J. Chem. Phys.* **1999**, 111, 2283.
16. H. Nishide, *Adv. Mater.* **1995**, 7, 937.

17. T. Kaneko, T. Matsubara, T. Aoki, *Chem. Mater.* **2002**, 14, 3898.
18. E. Dobrzyńska, M. Jouni, P. Gawryś, S. Gambarelli, J.-M. Mouesca, D. Djurado, L. Dubois, I. Wielgus, V. Maurel, I. Kulszewicz-Bajer, *J. Phys. Chem. B* **2012**, 116, 14968.
19. T. L. Makarova, B. Sundqvist, R. Höhne, P. Esquinazi, Y. Kopelevich, P. Scharff, V. A. Davydov, L. S. Kashevarova, A. V. Rakhmanina, *Nature* **2001**, 413, 716.
20. G. Z. Magda, X. Jin, I. Hagymási, P. Vancsó, Z. Osváth, P. Nemes-Incze, C. Hwang, L. P. Biró, L. Tapasztó, *Nature* **2014**, 514, 608.
21. X. L. Wu, R. S. Wang, J. Cheng, G. H. Zhong, X. J. Chen, Y. Gao, Z. B. Huang, *Carbon* **2018**, 136, 125.
22. Q. Jiang, J. Zhang, Z. Mao, Y. Yao, D. Zhao, Y. Jia, D. Hu, Y. Ma, *Adv. Mater.* **2022**, 34, 2108103.
23. J. Mahmood, J. Park, D. Shin, H.-J. Choi, J.-M. Seo, J.-W. Yoo, J.-B. Baek, *Chem* **2018**, 4, 2357.
24. H. Phan, T. S. Herng, D. Wang, X. Li, W. Zeng, J. Ding, K. P. Loh, A. T. Shen Wee, J. Wu, *Chem* **2019**, 5, 1223.
25. S. Wu, M. Li, H. Phan, D. Wang, T. S. Herng, J. Ding, Z. Lu, J. Wu, *Angew. Chem. Int. Ed.* **2018**, 57, 8007.
26. J. Mahmood, J. B. Baek, *Chem* **2019**, 5, 1012.
27. K. Sakaushi, M. Antonietti, *Acc. Chem. Res.* **2015**, 48, 1591.
28. E. Jin, M. Asada, Q. Xu, S. Dalapati, M. A. Addicoat, M. A. Brady, H. Xu, T. Nakamura, T. Heine, Q. Chen, D. Jiang, *Science* **2017**, 357, 673.

29. K. S. Burch, D. Mandrus, J.-G. Park, *Nature* **2018**, 563, 47.

30. M. Wei, K. Song, Y. Yang, Q. Huang, Y. Tian, X. Hao, W. Qin, *Adv. Mater.* **2020**, 32, 2003293.

31. W. P. Su, J. R. Schrieffer, A. J. Heeger, *Phys. Rev. Lett.* **1979**, 42, 1698.

32. H. Fukutome, A. Takahashi, M.-a. Ozaki, *Chem. Phys. Lett.* **1987**, 133, 34.

33. S. Ramasesha, B. Sinha, *Chem. Phys. Lett.* **1991**, 179, 379.

34. H. Nishide, N. Yoshioka, T. Kaneko, E. Tsuchida, *Macromolecules* **1990**, 23, 4487.

35. A. Fujii, T. Ishida, N. Koga, H. Iwamura, *Macromolecules* **1991**, 24, 1077.

36. R. Saf, K. Hummel, K. Gatterer, H. P. Fritzer, *Polym. Bull.* **1992**, 28, 395.

37. H. Nishide, T. Kaneko, N. Yoshioka, H. Akiyama, M. Igarashi, E. Tsuchida, *Macromolecules* **1993**, 26, 4567.

38. H. Murata, D. Miyajima, R. Takada, H. Nishide, *Polym J* **2005**, 37, 818.

39. T. Itoh, Y. Jinbo, K. Hirai, H. Tomioka, *J. Am. Chem. Soc.* **2005**, 127, 1650.

40. M. F. Beristain, M. F. Jimenez-Solomon, A. Ortega, R. Escudero, E. Muñoz, Y. Maekawa, H. Koshikawa, T. Ogawa, *Mater. Chem. Phys.* **2012**, 136, 1116.

41. Y. S. Gal, S. H. Jin, S. K. Choi, *J Mol Catal A-chem* **2004**, 213, 115.

42. M. G. Mayershofer, O. Nuyken, M. R. Buchmeiser, *Macromolecules* **2006**, 39, 3484.

43. F. Yang, Z. Zhang, M. Chen, H. Zhang, J. Zhang, J. Z. Sun, *Polym. Chem.* **2022**, 13, 6492.